Histol Histopathol (2014) 29: 1039-1046
DOI: 10.14670/HH-29.1039

http://www.hh.um.es

Histology and Histopathology
Cellular and Molecular Biology

Distribution of dendritic cells expressing dendritic cell-specific ICAM-3-grabbing non-integrin (DC-SIGN, CD209): Morphological analysis using a novel Photoshop-aided multiple immunohistochemistry technique

Akihiro Masuda and Toshio Nishikawa
Department of Surgical Pathology, Tokyo Women's Medical University, Tokyo, Japan

Summary. The distribution of dendritic cells (DCs) expressing DC-specific ICAM-3-grabbing non-integrin (DC-SIGN, CD209) and the morphological interaction of DC-SIGN$^+$ DCs with other cells, especially B cells, in tonsillar and other lymphoid tissues were investigated by multiple immunohistochemistry (IHC) using the graphics editing program Photoshop, which enabled staining with 4 or more antibodies in formalin-fixed paraffin sections. Images obtained by repetition of conventional IHC using diaminobenzidine color development in a tissue section were processed on Photoshop for multiple staining. DC-SIGN$^+$ DCs were present in the area around the lymphoid follicles and formed a DC-SIGN$^+$ DC-rich area, and these cells contacted not only T cells, fascin$^+$ DCs, and blood vessels but also several subsets of B cells simultaneously, including naïve and memory B cells. DC-SIGN$^+$ DCs may play an important role in the regulation of the immune response mediated by not only T cells but also B cells. The multiple IHC method introduced in the present study is a simple and useful method for analyzing details of complex structures. Because this method can be applied to routinely processed paraffin sections with conventional IHC with diaminobenzidine, it can be applied to a wide variety of archival specimens.

Key words: Multiple immunohistochemistry, Dendritic cells, DC-SIGN, B cell, Photoshop

Offprint requests to: Akihiro Masuda, Department of Surgical Pathology, Tokyo Women's Medical University, 8-1 Kawada-chou, Shinjuku-ku, Tokyo, 162-8666, Japan. e-mail: masuda@cat.email.ne.jp

Introduction

Dendritic cells (DCs) are professional antigen (Ag)-presenting cells that stimulate Ag-specific resting naïve T cells to proliferate (Banchereau et al., 2000). DCs have several subsets, and one of these subsets expresses DC-specific ICAM-3-grabbing non-integrin (DC-SIGN, CD209) (Geijtenbeek et al., 2000), which facilitates migration of DCs from blood into tissue and mediates DC-T cell clustering necessary for an efficient immune response (Geijtenbeek et al., 2002). Moreover, DC-SIGN binds to several pathogens and contributes to HIV transmission (Geijtenbeek et al., 2000; Geijtenbeck and van Kooyk, 2003). In lymph nodes, DC-SIGN expression is restricted to a subset of DCs (Engering et al., 2004). Although DC-SIGN$^+$ DCs have been identified in the T cell area and outer cortex in proximity to sinuses of lymph nodes, DC-SIGN is predominantly expressed by macrophages in the medulla (Granelli-Piperno et al., 2005). DC-SIGN$^+$ DCs are also present in the interfollicular region of Peyer's patch (Jameson et al., 2002). Although DC-SIGN$^+$ DC have been observed in the tonsils (Geijtenbeek et al., 2000), details of their distribution are largely unknown.

In lymph nodes, DCs expressing low levels of DC-SIGN appear to neighbor the lymphoid follicles (Angel et al., 2009). In our previous study on DC-SIGN$^+$ cell distribution in the lymphoid stroma of Warthin's tumor (Masuda et al., 2006), DC-SIGN$^+$ DCs were predominant in the periphery of the T cell areas and constituted a DC-SIGN$^+$ DC-rich area, although a small number of DC-SIGN$^+$ cells was observed in the sinus structure remnant in the lymphoid stroma. In the DC-

SIGN+ DC-rich area of the lymphoid stroma of Warthin's tumor, both B cells and T cells are present (Masuda et al., 2006), which suggests a close relationship of DC-SIGN+ DCs not only to T cells but also to B cells. Although several aspects of DC-B cell interaction have been reported (Banchereau et al., 2000), the morphological relationship of DC-SIGN+ DCs and B cells is largely unknown. These aspects prompted us to investigate the details of the DC-SIGN+ DC distribution and the anatomical relationship of DC-SIGN+ DCs to lymphocyte subsets, especially those of B cells, in secondary and tertiary lymphoid tissues.

To investigate the microanatomy of a complex structure such as lymphoid tissue by using immunohistochemistry (IHC), multiple IHC is essential. Given the advantage of precise morphological evaluation and availability of abundant archival specimens, it is desirable to use formalin-fixed paraffin sections. However, multiple staining of more than 3 colors using enzymatic IHC on paraffin sections has never been considered practical. We have reported a double-staining method that can be applied to paraffin sections by using the image stack function of the graphics editing program Adobe Photoshop, by which clear results for double IHC can be obtained (Masuda et al., 2008). In the present study, we adopted this method for staining with at least 4 antibodies and applied it to the investigation of the DC-SIGN+ DC distribution and the relationship of DC-SIGN+ DCs to lymphocyte subsets in tonsillar lymphoid tissue as well as other secondary and tertiary lymphoid tissues.

Materials and methods

Tissues

Tissue samples were obtained from the archives of the Department of Surgical Pathology at Tokyo Women's Medical University (Tokyo, Japan). Routinely processed formalin-fixed and paraffin-embedded materials of 8 cases of chronic tonsillitis (patients' mean age, 28.6 years; range, 6-44 years) were used. Five cases of mesenteric lymph nodes (obtained from gastrointestinal malignancy patients: mean age, 58.4 years; range, 47-73 years), 4 cases of appendix (phlegmonous appendicitis with hyperplasia of lymphoid apparatus: mean age, 25.3 years; range, 18-29 years), 5 cases of Warthin's tumor (mean age, 57 years; range, 51-67 years) and 5 cases of lymphocytic thyroiditis (without Hashimoto disease: mean age, 44.4 years; range, 29-62 years) were also analyzed.

Immunohistochemistry

Deparaffinized sections were treated with Dako REAL™ (DakoCytomation, Glostrup, Denmark) for blockade of intrinsic peroxidase, and then 2-step IHC was performed using goat anti-mouse immunoglobulin conjugated to peroxidase-labeled polymer (EnVision™, Dako) and diaminobenzidine (DAB) as the chromogen. The monoclonal antibodies (Abs) used in the present study were anti-DC-SIGN (R&D Systems, Minneapolis, MN), anti-CD23 (Nichirei Biosciences, Tokyo, Japan), anti-fascin (55-K2, DAKO), anti-CD3 (F7.2.38, DAKO), anti-CD20 (L26, DAKO), anti-CD34 Class II (QBEnd 10, DAKO), anti-CD27 (137B4, Leica Microsystems, Wetzlar, Germany), anti-CD79a (JCB117, DAKO), anti-Ki-67 (MIB-1, DAKO), and anti-IgD (IgD26, DAKO). Hematoxylin staining for nuclei was performed after development. Photomicrographs of the stained tissues were digitally taken using a standard microscope and a digital photo system. The cover glass of the slide was removed, and the same IHC procedure was applied for the next Ab. Digital photomicrographs of microscopical fields identical to those of the previous step staining were obtained. An Olympus BX41 microscope equipped with an Olympus C-5060 digital camera (Olympus, Tokyo, Japan) was used in the present study. The same procedure for IHC was performed for the third, fourth and fifth Abs.

Double staining using photoshop

A detailed method to obtain images for double staining has already been reported (Masuda et al., 2008). The method is based on acquisition of an individual positive color by obtaining the difference of 2 images of an identical microscopic field, one showing the distribution of the first-stained Ag and the other showing the distribution of both the first- and second-stained Ags. To obtain the difference, image stack and blending mode functions of Photoshop were used. Two images were opened in Photoshop (CS3, Adobe systems, San Jose, CA) and combined into 1 multi-layered image by using a script (found under Choose File > Scripts > Load Files into Stack). The layers of images were then aligned by creating an image stack (found under Edit > Auto-Align Layers, and select Auto as the alignment option). To distinguish between the same DAB brown color for 2 different Ags, manipulation of each layer of this 2-layer image was performed. First, the brown color in 1 layer was changed into a color that can be distinguished easily from the brown color. Changing of color was accomplished using the "Adjust hue" and saturation command (found under Image > Color adjustment). The blending mode "Darken" or "Darker Color" (found in the Layers palette) was applied to the upper layer to obtain a clear image of double IHC.

Multiple staining on photoshop, color range command method and difference mode method

Although double staining is easily performed using the above-mentioned method, it is difficult to obtain clear images of multiple staining with more than 3 colors with a simple repetition of the method. This difficulty is partly attributable to the characteristics of the blending modes. The blending modes work based on the RGB

color model (see Photoshop manufacturer's instruction). In Darken mode, pixels lighter than the blend color are replaced, and pixels darker than the blend color do not change. Hence, this mode produces a third color. In contrast, Darker Color mode compares the total of all channel values for the blend and base color and displays the lower-value color. Hence, it does not produce a third color. In either method, simple repetition makes the images too dark to be analyzed. Hence, to compose images of staining with more than 3 colors, it is necessary to acquire an individual positive color for each Ag and superimpose the colors (Fig. 1, see also legends). This method is also based on acquisition of an individual positive color by obtaining the difference of 2 images. To obtain the difference, the eyedropper pointer was used over the positive area of an image of double IHC. Then, the color range command was applied to select the specific color acquired by the eyedropper pointer, and the range of colors was selected using the fuzziness slider on the selection preview display. Accurate positive areas were determined by viewing the areas that appeared in the selection preview display. The Select > Inverse, and Edit > Cut functions were then chosen to acquire the positive area for the second Ag, which was then superimposed onto the image obtained with the first Ag. Because this procedure (named the "color range command method") does not produce a third color, the shapes of the positive areas are similar to those of areas

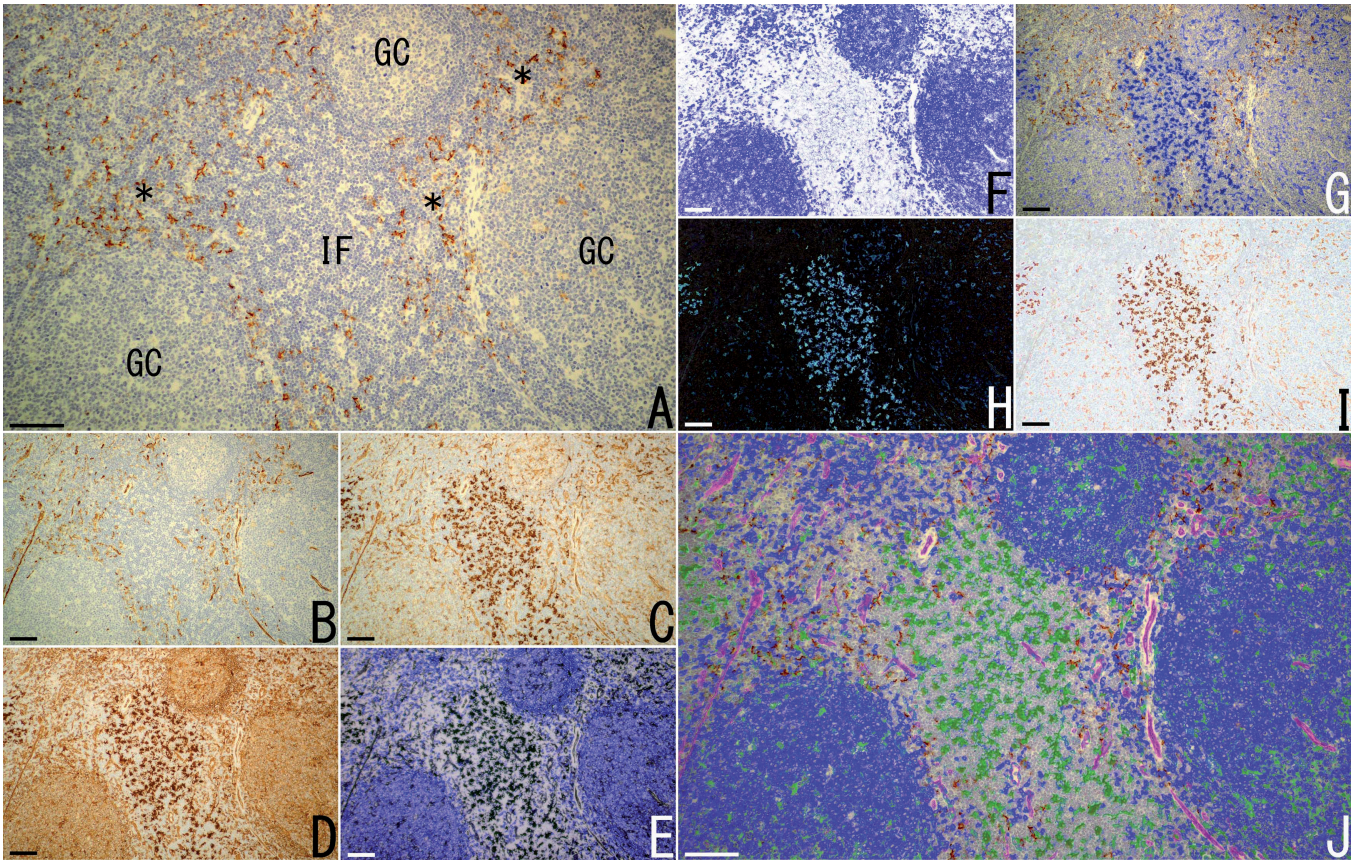

Fig. 1. DC-SIGN$^+$ DC distribution in the tonsil and the multiple staining procedures (see Materials and Methods). **A.** Single immunohistochemistry (IHC) of the tonsil for DC-SIGN. DC-SIGN$^+$ DCs are observed in areas among lymphoid follicles with germinal centers (GC) and interfollicular areas (IF), and they form DC-SIGN$^+$ DC areas (*). **B.** The identical microscopic field from the same histological section as shown in 1A is shown, after additional CD34 IHC. Both DC-SIGN$^+$ DCs and CD34$^+$ blood vessels are stained with the same brown color. **C.** The identical microscopic field of the same histological section as shown in A and B is shown, after additional fascin IHC. **D.** The same microscopic field of the same histological section as shown in A, B, and C is shown, after additional CD79a IHC. **E.** The figure panels for the same microscopic field of the same histological section **(A to D)** are combined into a multi-layered image and aligned on Photoshop. Only layers C and D are visible in this figure (active on the Layer palette) to highlight CD79a$^+$ cells. The diaminobenzidine color in layer C was changed using Darken mode (blue for CD79a and black for the other three Abs). **F.** The CD79a$^+$ chromogen color was acquired from Fig. 1E by using the color range command method. **G.** Fig. 1A and the fascin-positive chromogen color acquired by the color range command method are combined (brown for DC-SIGN and blue for fascin). **H.** Layers of Figs. 1B and 1C where the difference mode method is applied to obtain only the chromogen color for fascin. Fascin$^+$ cells are highlighted in silver. **I.** Inverted image of Fig. 1H, showing fascin in its original brown color. **J.** A complete quadruple IHC figure. Figs. 1A to 1D were combined using the color range command method (brown for DC-SIGN, fuchsia for CD34, green for fascin and blue for CD79a). Scale bar: 100 μm.

in the above-mentioned double staining procedure using Darker Color blending mode. The blending mode "difference" (found in the Layers palette) was also used to acquire positive areas for each Ag; it was applied to the upper layer, and the acquired image was inverted using the Invert command (found under Image > Adjustments) to obtain the original brown color image and superimpose it with an appropriate blending mode (named the "difference mode method").

Heat treatment

Ag retrieval using Target Retrieval Solution, pH9 (DAKO) in a Pascal pressure chamber (DAKO) (125°C, 40 min) was performed. Although cross reactivity does not need to be considered for the method described in the present study, heat treatment was performed before each staining. The intensity of the DAB color for the second Ag, processed without heat treatment after staining for the first Ag, was weaker than that of the color processed with heat treatment (data not shown), which suggests that the remaining Ag-binding sites on the goat anti-mouse immunoglobulin conjugated to peroxidase-labeled polymer may decrease the stainability of the second Ag and that heat treatment may disable the Ag-binding sites.

Results

Single IHC for DC-SIGN in the tonsil showed that cells with thin dendritic processes positive for DC-SIGN were present in the area surrounding lymphoid follicles, and appeared to form DC-SIGN$^+$ DC-rich areas (Fig. 1A). Multiple IHC with anti-DC-SIGN, anti-fascin, anti-CD34, and anti-CD79a in the same field of the same histological section as shown in Fig. 1A (Fig. 1J) revealed that DC-SIGN$^+$ DC-rich areas were located in the periphery of fascin$^+$ DC-rich interfollicular areas. DCs showing a strong diffuse cytoplasmic staining pattern of fascin are considered to be mature DCs and to be equivalent to interdigitating DCs in the paracortex of the lymph nodes (Pinkus et al., 1997). Although these DCs were also located in the DC-SIGN$^+$ DC-rich area, they were more prevalent in central T cell areas. In DC-

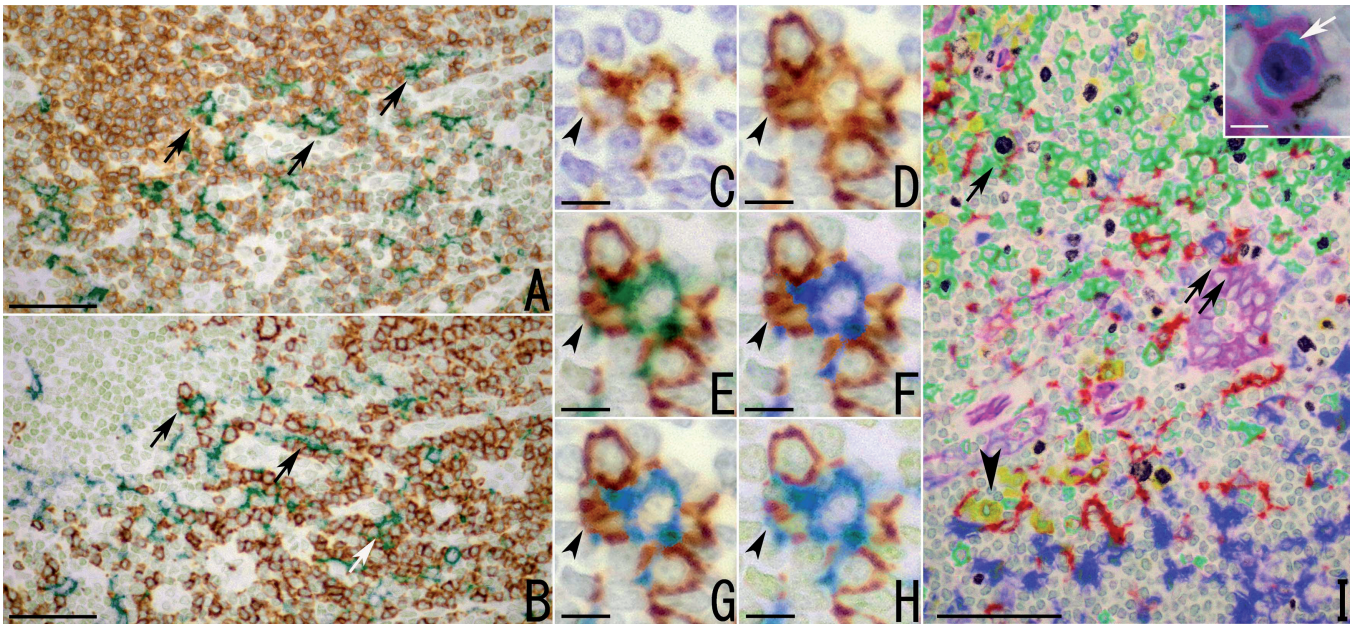

Fig. 2. DC-SIGN$^+$ DCs, CD20$^+$ B cells and CD3$^+$ T cells in the tonsil: **(A)** In the periphery of the T cell areas, DC-SIGN$^+$ DCs contact CD3$^+$ T cells (arrow) (green for DC-SIGN, brown for CD3), and **(B)** they also directly contact CD20$^+$ B cells and form clusters with them (arrow) (green for DC-SIGN, brown for CD20). A and B are semi-serial sections. **C to H.** High-power view of DC-SIGN$^+$ DCs-CD20$^+$ B cell-clusters using various blending and superimposing methods (see Materials and Methods). DC-SIGN IHC **(C)** and DC-SIGN with additional CD20 IHC **(D)** are combined into double-layer images with the blending mode Darken **(E)**, the blending mode Darker color **(F)**, DC-SIGN color acquired by the color range command method and superimposed on Fig. **2D (G),** and CD20 color acquired by the difference mode method and superimposed on Fig. 2C **(H)**. Although it is clear that DC-SIGN$^+$ DCs and their cytoplasmic processes (blue or green) contact CD20$^+$ B cells (brown), each method is different with regard to areas where chromogen precipitation overlaps. Weakly positive cytoplasmic processes may disappear (arrows in **C to H**). **I.** High-power view of 6-color multiple staining of the DC-SIGN$^+$ DC-rich area of the tonsil with a combination of the color range command method and the difference mode method (red for DC-SIGN, black for Ki-67, fuchsia for CD34, blue for fascin and green for CD20, yellow for CD79a). Cytoplasmic processes of DC-SIGN$^+$ DC contact Ki-67$^+$CD20$^+$ cells (arrow), CD34$^+$ blood vessels (paired arrows), and both fascin$^+$ cells and CD20$^-$CD79a$^+$ cells (arrow head). The inset of (I) shows a higher magnification of this Ki-67$^+$CD20$^+$ cell with different color assignment, and clearly shows intracytoplasmic staining of CD79a (aqua blue) with surface staining of CD20 (fuchsia) and nuclear staining of Ki-67 (purple). Scale bars: A, B, I, 100 μm; C-H, 10 μm; inset of I, 5 μm.

SIGN$^+$ DC-rich areas, CD79a$^+$ B cells and CD34$^+$ blood vessels were also observed. Relatively few DC-SIGN$^+$ cells were observed in the T cell areas where cells intensely positive for fascin were observed. Fig. 1 also shows the detailed multiple staining methods using Photoshop (see Materials and Methods and figure legends).

Double staining of CD3 and DC-SIGN and that of CD20 and DC-SIGN revealed that both CD3$^+$ T cells and CD20$^+$ B cells contacted DC-SIGN$^+$ DCs in the DC-SIGN$^+$ DC-rich area of the tonsil (Fig. 2). A high-power view of the double staining of CD20 and DC-SIGN showed that DC-SIGN$^+$ DCs formed clusters with CD20$^+$ B cells and the extended cytoplasmic processes of DC-SIGN$^+$ DCs also contacted CD20$^+$ B cells (Figs. 2E to 2H). Fig. 2 also shows the difference between the blending and superimposing methods on Photoshop. The boundary of positive areas obtained using the Darken blending mode (Fig. 2E) was different from that obtained using the Darker Color blending mode (Fig. 2F) or the color range command method (Fig. 2G). Although clear boundaries between positive areas were obtained with the Darker Color mode and the color range command method, some positive areas observed in single IHC staining and Darken mode vanished when these methods were used. Although the difference mode method was simpler than the color range command method, some positive areas were not fully obtained (Fig. 2H).

Because a close relationship between B cells and DC-SIGN$^+$ DCs was observed in DC-SIGN$^+$ DC-rich area, we next investigated the B cell subsets that form clusters with DC-SIGN$^+$ DCs. First, multiple staining, including that of CD20 and CD79a, was performed. In the procedure of the image shown in Fig. 2I, CD79a staining was performed after CD20 staining. Hence, CD79a$^+$CD20$^-$ and cytoplasmic CD79a$^+$CD20$^+$ B cells were detected. In the DC-SIGN$^+$ DC-rich area of the tonsil, DC-SIGN$^+$ DCs contacted both CD20$^+$ B cells and CD79a$^+$CD20$^-$ B cells, which are considered to represent the final differentiation stage toward plasma cells. Contact of the thin cytoplasm of DC-SIGN$^+$DCs with Ki-67$^+$cytoplasmic CD79a$^+$CD20$^+$ B cells was also observed. Moreover, DC-SIGN$^+$ DCs contacted fascin$^+$ DCs and CD34$^+$ blood vessels. Multiple staining, including that of IgD and CD27, was then performed to determine the relationship of naïve and memory B cells to DC-SIGN$^+$ DCs, as CD27 is a reliable marker for memory B cells (Klein et al., 1998; Agematsu et al., 2000). Although relatively few IgD$^+$ B cells are CD27$^+$ memory cells, many IgD$^+$ B cells in the tonsil are naïve B cells (Bohnhorst et al., 2001). To detect IgD$^+$ cells and IgD$^-$CD27$^+$CD3$^-$ cells in the tonsil, CD27 staining was performed after staining for CD3 and IgD. DC-SIGN$^+$DCs simultaneously clustered with IgD$^+$ B cells, IgD$^-$CD27$^+$CD3$^-$ B cells, and CD3$^+$ T cells (Fig. 3). Staining for IgD was then performed after staining for CD3 and CD27 to detect CD27$^-$IgD$^+$ cells and CD27$^+$CD3$^-$ cells. DC-SIGN$^+$DCs also simultaneously clustered with CD27$^+$ B cells, CD27$^-$IgD$^+$ B cells, and CD3$^+$ T cells (data not shown). A very small number of CD23$^+$ B cells contacted DC-SIGN$^+$DCs (data not shown).

DC-SIGN$^+$ DCs were observed in the peripheral T cell zones of the lymphoid stroma of Warthin's tumor, appendicular lymphoid tissues, and lymphoid tissues in lymphocytic thyroditis, and they were found to contact CD20$^+$ B cells (Fig. 4). In the lymph nodes, DC-SIGN$^+$ DCs were also observed in T cell zones. Although the formation of DC-SIGN$^+$ DC rich areas was not as clear as in the tonsillar lymphoid tissue, DC-SIGN$^+$ DCs contacted CD20$^+$ B cells in the periphery of paracortex. Contact of DC-SIGN$^+$ DCs with CD27$^+$CD3$^-$ B cells, and CD3$^+$ T cells was also detected in these lymphoid

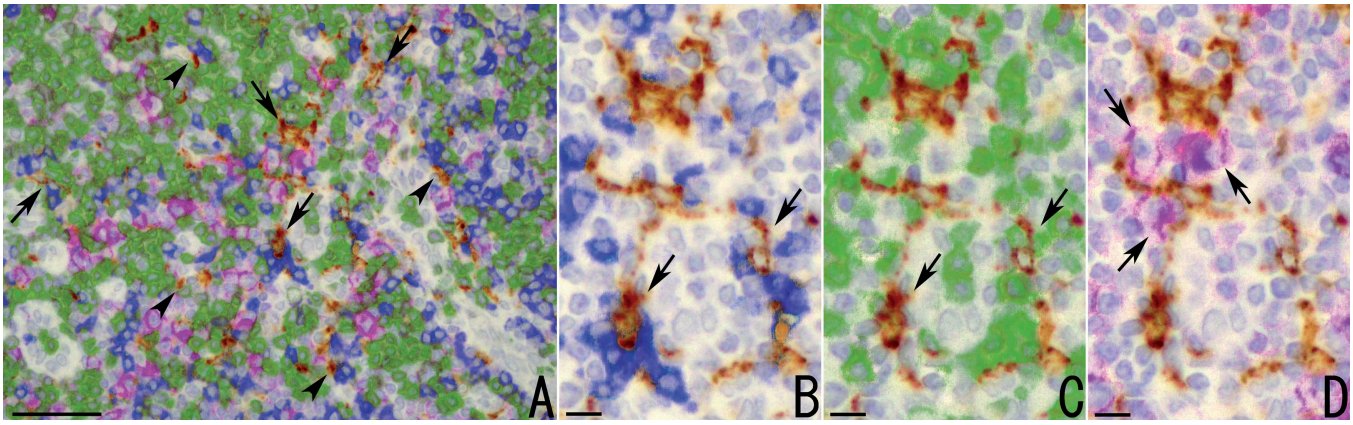

Fig. 3. A. Quadruple staining for DC-SIGN (brown), IgD (blue), CD3 (green), and CD27 (fuchsia) of the tonsil. Because CD27 IHC was performed after CD3 IHC, CD3$^+$ T cells, IgD$^+$ B cells and CD3$^-$CD27$^+$ B cells were detected. DC-SIGN$^+$ DCs and their cytoplasmic processes contact IgD$^+$ cells, CD3$^+$ cells and CD3$^-$CD27$^+$ cells simultaneously (arrow). **B-D.** High-power views of individual chromogen colors superimposed on a single DC-SIGN IHC image. DC-SIGN$^+$ DCs contact IgD$^+$ cells **(B)**, CD3$^+$ cells **(C)**, and CD3$^-$CD27$^+$ cells **(D)** simultaneously. Scale bars: A, 50 μm; B-D, 10 μm.

tissues (Fig. 4F,G).

Discussion

Precise interpretation of results is difficult in conventional enzymatic IHC for multiple staining of paraffin sections. The difficulty partly results from diffusion, co-staining and cross-reaction. However, the IHC procedure described in the present study makes multiple IHC in paraffin sections practical. The use of only standard IHC with DAB, with which a pinpoint Ag distribution can be obtained, is good for clear staining, and the acquisition of different images for different Ags is thought to make analysis easy. Moreover, because there is no concern over cross reactivity in this procedure, a sensitive multi-step IHC method such as the EnVision system can be applied multiple times. Although it has been reported that heat treatment generally blocks cross reactivity on double staining (Lan et al., 1995), there is still some concern about its possibility of cross reaction in conventional multiple staining protocols using multi-step IHC. The usage of multiple IHC on paraffin sections has several benefits: precise morphological evaluation can be performed and accumulated archival specimens can be easily analyzed. Moreover, IHC images can be superimposed precisely and easily on images of conventional hematoxylin-eosin staining or other staining types.

Several aspects must be considered in the procedure described in the present study, some of which also must be considered in conventional enzymatic IHC. First, double-positive cells cannot be detected unless the intracellular localization of the Ags is different. Steininger et al. (2005) reported the detection of $CD27^+$ B-cells by immunoenzymatic subtractive double-staining, in which they adopted an avidin-biotinylated alkaline phosphatase complex procedure that involved visualization in a dark blue color with nitroblue tetrazolium/bromo-chloro-indolyl phosphate for CD3, followed by an avidin-biotinylated peroxidase complex procedure that involved visualization in brown color using DAB for CD27. The procedure we introduced in the present study is useful for studies in which such a subtractive method is suitable. When the intracellular localization is different for each Ag, clear multiple staining images can be obtained using the IHC procedure described in the present study.

DAB precipitation on the cell surface may interfere

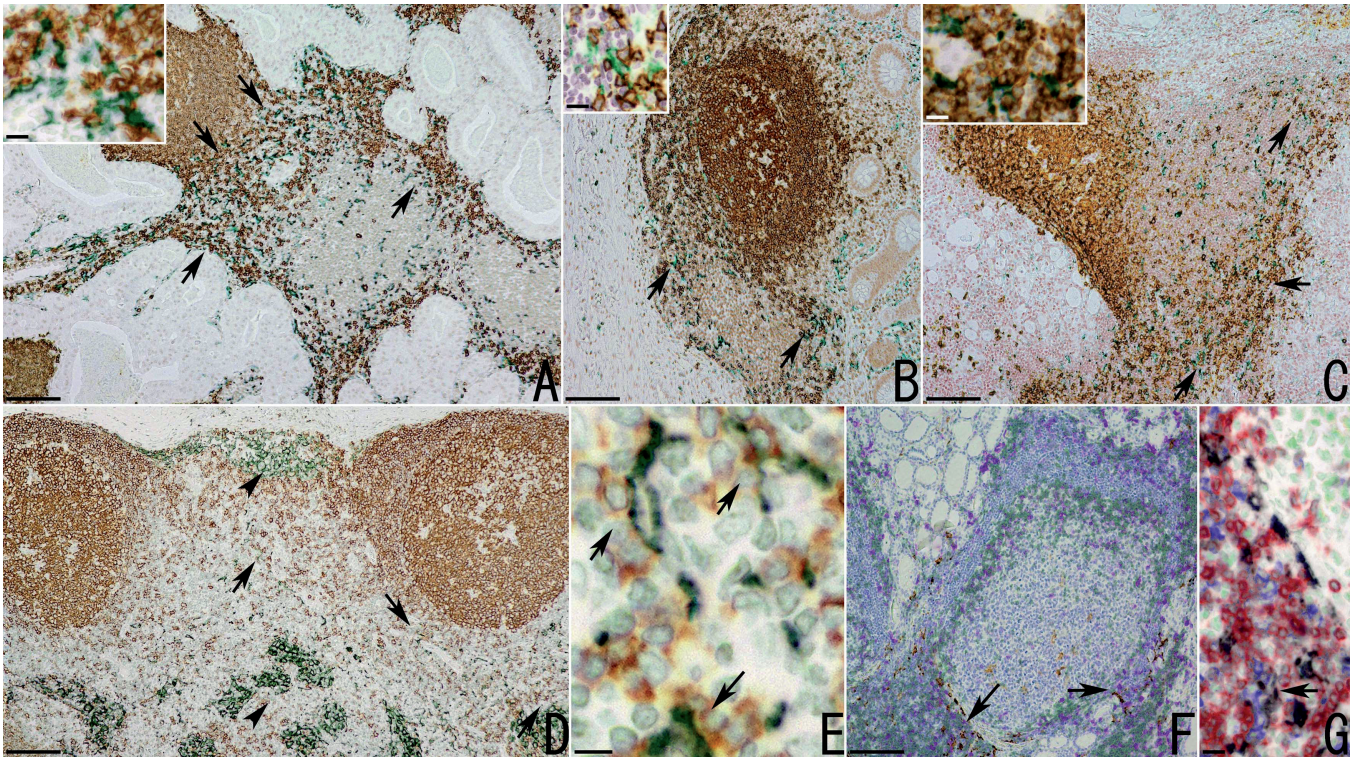

Fig. 4. Double staining of CD20 and DC-SIGN (green for DC-SIGN, brown for CD20) in Warthin's tumor **(A)**, appendix **(B)**, lymphocytic thyroiditis **(C)** and lymph node (**D and E**). Many B cells are observed in DC-$SIGN^+$ DC-rich areas (arrow). High power views (insets of A to C, and E) show that DC-$SIGN^+$ DCs and $CD20^+$ B cells form clusters. Macrophages in the sinuses of the lymph node are also positive for DC-SIGN (D, arrow head). In triple IHC of lymphocytic thyroiditis (**F and G**), because CD27 IHC was performed after CD3 IHC, $CD3^+$ T cells and $CD3^-CD27^+$ B cells were detected (F: brown for DC-SIGN, green for CD3, and purple for CD27; G: black for DC-SIGN, red for CD3, and blue for CD27). DC-$SIGN^+$ DCs simultaneously contacted $CD3^+$ T cells and $CD3^-CD27^+$ B cells around the lymphoid follicle (arrow). Scale bars: A-D, F, 100 μm; E, G, insets of A-C, 10 μm.

in the Ag-Ab reaction and/or the chromogen precipitation on the surface of adjacent cells in the next step of IHC. IHC for DC-SIGN, which is present on the thin cytoplasmic processes of a relatively small number of cells, should be performed before IHC for lymphocyte markers, which stain the densely packed cells around DCs, to allow DC-SIGN$^+$ cytoplasmic processes to be detected. Otherwise, the DC-SIGN$^+$ cytoplasmic processes would be overshadowed by the lymphocyte staining. Hence, careful consideration of the combination of Abs and the order of each step of IHC are necessary. In this regard, sections must be cut at the appropriate thickness.

It should be noted that processing of images on Photoshop may cause false-negative or false-positive results. Such errors may occur at any step of manipulation, and different superimposition methods give somewhat different images of multiple staining. Hence, the intensity of staining and the degree of non-specific staining should be considered by individually referring to the IHC results for each Ab, and photographs of the staining for each Ab must be carefully examined during Photoshop processing. Moreover, it must be emphasized that the ability to examine each step of staining on Photoshop is a unique advantage. Multiple staining results can be analyzed by comparing each layer of a multi-layer image on Photoshop using Layers palette function, in addition to evaluating the final multiple staining images.

Interactions between DCs and B cells have been shown to be important for many aspects of immunological reaction. Human interdigitating DCs directly stimulate CD40 to activate naïve B cells (Bjorck et al., 1997). B cell activation can be induced by Ag-carrying DCs around high endothelial venules before migration into the lymphoid follicles (Qi et al., 2006). DCs induce CD40-independent class switching (Litinskiy et al., 2002), and B cells regulate DC function (Moulin et al., 2000; Morva et al., 2012). Moreover, DCs can capture and retain unprocessed Ags and then transfer these Ags to naive B cells to initiate a specific Ab response (Wykes et al., 1998). Although the morphological interaction of interdigitating DCs with B cells in lymph nodes has been shown (Takahashi et al., 2001), the anatomical relationship of DC-SIGN$^+$ DC and B cells has not been investigated. Our study showed that DC-SIGN$^+$ DCs formed a DC-SIGN$^+$ DC-rich area around lymphoid follicles and contacted T cells, as well as several subsets of B cells, including naïve B cells and memory B cells. Because most B cells express ICAM3 (Cordell et al., 1994), the ICAM-3-DC-SIGN interaction may be involved in the contact of B cells with DC-SIGN$^+$ DCs. DC-SIGN$^+$ DCs in lymph node may also capture lymph-borne Ags and, on appropriate activation, migrate into the paracortex for Ag presentation to T cells (Engering et al., 2004). Although their molecular interactions are largely unknown, DC-SIGN$^+$ DCs may play an important role in the regulation of the immune response of B cells, and they may play an important role in the interaction of B cells and T cells in systemic lymphoid tissues. Moreover, because DC-SIGN$^+$ DCs contacted blood vessels and fascin$^+$ mature DCs, they may be involved in the regulation of the interaction of these cells.

In conclusion, we showed that in tonsils and other secondary and tertiary lymphoid tissues, DC-SIGN$^+$ DCs were present in the area around the lymphoid follicles and form a DC-SIGN$^+$ DC-rich area, and they simultaneously contacted not only T cells but also several subsets of B cells, by multiple IHC using Photoshop. The multiple IHC method we introduced in the present study is a simple and useful method for analyzing details of complex structures. Because this method can be applied to routinely processed paraffin sections using popular DAB IHC, it may be applied to a wide variety of specimens.

References

Agematsu K., Hokibara S., Nagumo H. and Komiyama A. (2000). CD27: a memory B-cell marker. Immunol. Today 21, 204-206.

Angel C.E., Chen C.J., Horlacher O.C., Winkler S., John T., Browning J., MacGregor D., Cebon J. and Dunbar P.R. (2009). Distinctive localization of antigen-presenting cells in human lymph nodes. Blood 113, 1257-1267.

Banchereau J., Briere F., Caux C., Davoust J., Lebecque S., Liu Y.J., Pulendran B. and Palucka K. (2000). Immunobiology of dendritic cells. Annu. Rev. Immunol. 18, 767-811.

Bjorck P., Flores-Romo L. and Liu Y.J. (1997). Human interdigitating dendritic cells directly stimulate CD40-activated naive B cells. Eur. J. Immunol. 27, 1266-1274.

Bohnhorst J.O., Bjorgan M.B., Thoen J.E., Natvig J.B. and Thompson K.M. (2001). Bm1-Bm5 classification of peripheral blood B cells reveals circulating germinal center founder cells in healthy individuals and disturbance in the B cell subpopulations in patients with primary Sjogren's syndrome. J. Immunol. 167, 3610-3618.

Cordell J.L., Pulford K., Turley H., Jones M., Micklem K., Doussis I.A., Tyler X., Mayne K., Gatter K.C. and Mason D.Y. (1994). Cellular distribution of human leucocyte adhesion molecule ICAM-3. J. Clin. Pathol. 47, 143-147.

Engering A., van Vliet S.J., Hebeda K., Jackson D.G., Prevo R., Singh S.K., Geijtenbeek T.B., van Krieken H. and van Kooyk Y. (2004). Dynamic populations of dendritic cell-specific ICAM-3 grabbing nonintegrin-positive immature dendritic cells and liver/lymph node-specific ICAM-3 grabbing nonintegrin-positive endothelial cells in the outer zones of the paracortex of human lymph nodes. Am. J. Pathol. 164, 1587-1595.

Geijtenbeek T.B. and van Kooyk Y. (2003). Pathogens target DC-SIGN to influence their fate DC-SIGN functions as a pathogen receptor with broad specificity. APMIS 111, 698-714.

Geijtenbeek T.B., Torensma R., van Vliet S.J., van Duijnhoven G.C., Adema G.J., van Kooyk Y. and Figdor C.G. (2000). Identification of DC-SIGN, a novel dendritic cell-specific ICAM-3 receptor that supports primary immune responses. Cell 100, 575-585.

Geijtenbeek T.B., Engering A. and van Kooyk Y. (2002). DC-SIGN, a C-type lectin on dendritic cells that unveils many aspects of dendritic cell biology. J. Leukoc. Biol. 71, 921-931.

Granelli-Piperno A., Pritsker A., Pack M., Shimeliovich I., Arrighi J.F.

Park C.G., Trumpfheller C., Piguet V., Moran T.M. and Steinman R.M. (2005). Dendritic cell-specific intercellular adhesion molecule 3-grabbing nonintegrin/CD209 is abundant on macrophages in the normal human lymph node and is not required for dendritic cell stimulation of the mixed leukocyte reaction. J. Immunol. 175, 4265-4273.

Jameson B., Baribaud F., Pohlmann S., Ghavimi D., Mortari F., Doms R.W. and Iwasaki A. (2002). Expression of DC-SIGN by dendritic cells of intestinal and genital mucosae in humans and rhesus macaques. J. Virol. 76, 1866-1875.

Klein U., Rajewsky K. and Kuppers R. (1998). Human immunoglobulin (Ig)M^+IgD^+ peripheral blood B cells expressing the CD27 cell surface antigen carry somatically mutated variable region genes: CD27 as a general marker for somatically mutated (memory) B cells. J. Exp. Med. 188, 1679-1689.

Lan H.Y., Mu W., Nikolic-Paterson D.J. and Atkins R.C. (1995). A novel, simple, reliable, and sensitive method for multiple immunoenzyme staining: use of microwave oven heating to block antibody crossreactivity and retrieve antigens. J. Histochem.Cytochem. 43, 97-102.

Litinskiy M.B., Nardelli B., Hilbert D.M., He B., Schaffer A., Casali P. and Cerutti A. (2002). DCs induce CD40-independent immunoglobulin class switching through BLyS and APRIL. Nat. Immunol. 3, 822-829.

Masuda A., Nishikawa T., Yamamoto T. and Kobayashi M. (2006). Distribution of DC-SIGN dendritic cells in the lymphoid stroma of Warthin's tumour; immunohistochemical analysis. Histopathology 49, 433-435.

Masuda A., Nishikawa T., Yamamoto T. and Kobayashi M. (2008). Simple method for Photoshop-aided double immunostaining - usage of 'image stack' function. Histopathology 53, 609-610.

Morva A., Lemoine S., Achour A., Pers J.O., Youinou P. and Jamin C. (2012). Maturation and function of human dendritic cells are regulated by B lymphocytes. Blood 119, 106-114.

Moulin V., Andris F., Thielemans K., Maliszewski C., Urbain J. and Moser M. (2000). B lymphocytes regulate dendritic cell (DC) function in vivo: increased interleukin 12 production by DCs from B cell-deficient mice results in T helper cell type 1 deviation. J. Exp. Med. 192, 475-482.

Pinkus G.S., Pinkus J.L., Langhoff E., Matsumura F., Yamashiro S., Mosialos G. and Said J.W. (1997). Fascin, a sensitive new marker for Reed-Sternberg cells of hodgkin's disease. Evidence for a dendritic or B cell derivation? Am. J. Pathol. 150, 543-562.

Qi H., Egen J.G., Huang A.Y. and Germain R.N. (2006). Extrafollicular activation of lymph node B cells by antigen-bearing dendritic cells. Science 312, 1672-1676.

Steiniger B., Timphus E.M., Jacob R. and Barth P.J. (2005). $CD27^+$ B cells in human lymphatic organs: re-evaluating the splenic marginal zone. Immunology 116, 429-442.

Takahashi K., Kenji A., Norihiro T., Eisaku K., Takashi O., Kazuhiko H., Tadashi Y. and Tadaatsu A. (2001). Morphological interactions of interdigitating dendritic cells with B and T cells in human mesenteric lymph nodes. Am. J. Pathol. 159, 131-138.

Wykes M., Pombo A., Jenkins C. and MacPherson G.G. (1998). Dendritic cells interact directly with naive B lymphocytes to transfer antigen and initiate class switching in a primary T-dependent response. J. Immunol. 161, 1313-1319.

Accepted February 12, 2014